Dynamics of a System of Two Coupled Kicked Rotors

A Thesis

submitted to
Indian Institute of Science Education and Research Pune
in partial fulfillment of the requirements for the
BS-MS Dual Degree Programme

by

Rushil Bala

Indian Institute of Science Education and Research Pune
Dr. Homi Bhabha Road,
Pashan, Pune 411008, INDIA.

May, 2019

Supervisor: Dr. M S Santhanam

Certificate

This is to certify that this dissertation entitled Dynamics of a System of Two Coupled Kicked Rotors towards the partial fulfilment of the BS-MS dual degree programme at the Indian Institute of Science Education and Research, Pune represents study/work carried out by Rushil Bala at Indian Institute of Science Education and Research under the supervision of Dr. M S Santhanam, Associate Professor, Department of Physics , during the academic year 2018-2019.

Dr. M S Santhanam

Committee:

Dr. M S Santhanam

Dr. Umakant Rapol

This thesis is dedicated to my parents.

Declaration

I hereby declare that the matter embodied in the report entitled Dynamics of a System of Two Coupled Kicked Rotors are the results of the work carried out by me at the Department of Physics, Indian Institute of Science Education and Research, Pune, under the supervision of Dr. M S Santhanam and the same has not been submitted elsewhere for any other degree.

Rushil Bala

Acknowledgements

Firstly, I thank Dr. M S Santhanam for being an excellent guide. He has been patient, accommodative and encouraging and I am truly indebted to him for making this project a wonderful experience. Secondly, I thank my friends for providing the help that I needed. I acknowledge the INSPIRE Scholarship that I have been receiving from the Department of Science and Technology, Government of India.

Abstract

Localization of interacting many-body quantum systems i.e. many-body localisation (MBL), is a topic of current interest. The kicked rotor system is a paradigmatic model of chaos and the quantum kicked rotor system is not only a tool to study MBL in other quantum systems, but is itself, experimentally realizable. Less progress has been made in the study of a system of coupled kicked rotors. In this thesis, the aim is to study the indicators of MBL in a variant of a system of two coupled kicked rotors.

Contents

Chapter 1

Invitation to Quantum Chaos

Natural systems exhibit chaotic behaviour which can be sourced to the non-linearity of the description of their dynamics. A system is deterministic if its dynamics can be described mathematically. Intuitively, the loss of predictability of the dynamics of a system is associated with chaos. It is important to note that determinism does not equate to predictability. "Deterministic chaos" is the study of the chaotic behaviour exhibited by deterministic systems. Deterministic chaos originated from the efforts of Henri Poincaré towards obtaining an analytical solution to the three-body problem. Since then, deterministic chaos has been a popular topic of scientific research. Consequently, it has been well understood that even simple deterministic natural systems can exhibit chaotic behaviour. Aided by the fast growth of computing facilities/capabilities, the authenticity and ubiquity of deterministic chaos has been appreciated across scientific disciplines.

In the context of classical mechanics (classically), if a system exhibits chaotic behaviour, then two trajectories describing its dynamics, originating at two neighbouring point in its phase space, will diverge exponentially with time. "The dynamics of the system is extremely sensitive to its initial conditions."

According to Bohr's correspondence principle, classical physics emerges as the $\hbar \to 0$ limit of quantum physics. Therefore, it would not be surprising if quantum systems fundamentally exhibited chaotic behaviour. However, the Schrödinger equation describing the dynamics of a quantum system is linear i.e. it does not uphold the extreme sensitivity of the dynamics of the quantum system to its initial conditions. Moreover, the concept of trajectories describing

the dynamics of a quantum system in its phase space, is undefined in quantum mechanics due to Heisenberg's uncertainty principle. Therefore, it is not sensible to develop a mathematical theory of chaos in the context of quantum mechanics like it has been done classically. One can then ask the question: "Is there a quantum analogue of classically deterministic chaos?"

This question was seriously revisited only after the development of semi-classical mechanics by M Gutzwiller and M V Berry. Although many physicists have studied the chaotic behaviour of quantum systems, there yet does not exist a mathematical theory of chaos in the context of quantum mechanics. What is now referred to as "quantum chaos" is truly, the study of the dynamics of quantum systems whose classical analogues exhibit chaotic behaviour. M V Berry preferred the phrase "quantum chaology" over quantum chaos, since the object under investigation was the presence of "universal signatures" in quantum systems whose classical analogues exhibited chaotic behaviour, that typical quantum systems did not have. Nevertheless, it is a study that endeavours to find a relation between classically deterministic chaos and quantum mechanics.

Chapter 2

Preliminary Concepts

A deterministic system that can be described by a Hamiltonian is a Hamiltonian system. The phase space of a Hamiltonian system $\mathcal{S}$ that has d degrees of freedom (DOF) is $2d$ dimensional; labelled by its canonical position and momentum variables q_i and p_i respectively. The Hamilton's equations of motion describing its dynamics are:

$$\dot{p}_i = -\frac{\partial H}{\partial q_i}; \quad \dot{q}_i = \frac{\partial H}{\partial p_i}$$

If $\mathcal{S}$ is conservative, then H is independent of time. If $\mathcal{S}$ is conservative, then its energy $E = H$ is constant (constant of motion). Moreover, E corresponds to a surface in the phase space of $\mathcal{S}$ on which its dynamics is restricted.

Visualization of the dynamics of $\mathcal{S}$ in its phase space is simplified by studying Poincaré surface sections. Instead of studying the dynamics of $\mathcal{S}$ restricted on the surface in its phase space corresponding to a constant of its motion, its dynamics on the intersection of this surface and a surface having a lower dimension is studied. Consider a Hamiltonian system that has 2 DOF. Its phase space is 4 dimensional. The dynamics of this system is studied with mappings between intersection points of a trajectory of its dynamics and the chosen surface section, in its phase space. In the case of a periodically kicked Hamiltonian system that has 1 DOF, there exists a mapping between two such intersection points that differ with time by the kicking time period. This is an example of a stroboscopic area-preserving map.

Every deterministic system has a flow map from its phase space to its phase space. A

deterministic system is volume-preserving if the volume of a set in its phase space is invariant under its flow map. Every Hamiltonian system is volume-preserving (Liouville's theorem). The Poincaré recurrence theorem states that certain volume-preserving deterministic systems will eventually return to a state very close to their initial states. This implies that a trajectory describing the dynamics of such a system in its phase space will eventually return to the neighbourhood of its initial point. The Poincaré recurrence time T_r is the length of time until this (first) return. The volume of this neighbourhood is finite in numerical calculations and its decrease causes computational difficulties. For systems exhibiting chaotic mixing, for sufficiently large Poincaré recurrence times: $P(T_r) \propto e^{-T_r}$ [1].

Refer to [2][3] for a more detailed presentation of the theory of dynamical systems.

Floquet Theory

Deterministic natural systems can exhibit chaotic behaviour when they are acted upon by a time-dependent force (driven systems). Driven systems undergo a transition of state from a regime in which they exhibit regular behaviour to a regime in which they exhibit chaotic behaviour. In the class of driven systems are periodically kicked Hamiltonian systems. These systems have discrete time-translation invariance and the quantum analogues of some of these systems, exhibit regular behaviour, during and after the aforementioned transition of state.

Consider a Hamiltonian system $\mathcal{S}$ descried by the Hamiltonian:

$$H(t) = H_0 + V(t)$$

where H_0 is its time-independent part and $V(t)$ is its time-dependent part. The Hamiltonian describing quantum $\mathcal{S}$ is:

$$\hat{H}(t) = \hat{H}_0 + \hat{V}(t)$$

The Schrödinger equation describing the dynamics of quantum $\mathcal{S}$ is:

$$i\hbar\frac{\partial}{\partial t}\left|\psi(t)\right\rangle = \mathbf{H}(t)\left|\psi(t)\right\rangle; \quad \mathbf{H}(t) = \mathbf{H}_0 + \mathbf{V}(t) \tag{2.1}$$

Let:

$$\hat{V}(t + s\tau) = \hat{V}(t) \qquad (\forall s \in \mathbb{Z})$$

Assumption: the following vectors are solutions of 2.

$$|\psi_\alpha(t)\rangle = e^{-\frac{i\Omega_\alpha t}{\hbar}} |\Phi_\alpha(t)\rangle$$

where

$$|\Phi_\alpha(t + s\tau)\rangle = |\Phi_\alpha(t)\rangle \,. \qquad (s \in \mathbb{Z})$$

Define:

$$\hat{H}_F \coloneqq \hat{H}(t) - i\hbar\frac{\partial}{\partial t}$$

Then:

$$\mathbf{H}_F |\Phi_\alpha(t)\rangle = \Omega_\alpha |\Phi_\alpha(t)\rangle$$

Therefore, $|\Phi_\alpha(t)\rangle$ is the α^{th} eigenstate of $\mathbf{H}_F$ whose corresponding eigenvalue is Ω_α. Every Ω_α is real since $\mathbf{H}_F$ is hermitian. Moreover, these eigenstates are orthonormal and form a complete basis for the Hilbert space of quantum $\mathcal{S}$. Therefore:

$$|\psi(t)\rangle = \sum_\alpha A_\alpha e^{-\frac{i\Omega_\alpha t}{\hbar}} |\Phi_\alpha(t)\rangle \,; \quad A_\alpha = \langle\Phi_\alpha(0)|\psi(0)\rangle$$

$$|\psi(t)\rangle = \sum_\alpha e^{-\frac{i\Omega_\alpha t}{\hbar}} |\Phi_\alpha(t)\rangle \langle\Phi_\alpha(0)|\psi(0)\rangle$$
$$|\psi(\tau)\rangle = \sum_\alpha e^{-\frac{i\Omega_\alpha \tau}{\hbar}} |\Phi_\alpha(0)\rangle \langle\Phi_\alpha(0)|\psi(0)\rangle$$

Let $\{|m\rangle\}$ be a complete set of orthonormal eigenstates of $\mathbf{H}_0$. Let $\psi_m(t) = \langle m|\psi(t)\rangle$. Then:

$$\psi_m(\tau) = \sum_n \mathbf{U}_{mn}(\tau)\psi_n(0)$$

where $\mathbf{U}(\tau)$ is the Floquet matrix of quantum $\mathcal{S}$ and:

$$\mathbf{U}_{mn}(\tau) = \sum_\alpha e^{-\frac{i\Omega_\alpha \tau}{\hbar}} \langle m|\Phi_\alpha(0)\rangle \langle\Phi_\alpha(0)|n\rangle$$

Once $\mathbf{U}(\tau)$ is obtained, then $\psi_n(N\tau)$ can be obtained:

$$\psi_n(N\tau) = \sum_m [(\mathbf{U}(\tau))^N]_{nm}\psi_m(0) \qquad (N \in \mathbb{N})$$

Succinctly:

$$|\psi(N\tau)\rangle = [\mathbf{U}(\tau)]^N |\psi(0)\rangle$$

Random Matrix Theory

A class of quantum Hamiltonian systems that have no classical analogues are the compound nuclei of atoms. These systems have the earlier mentioned "universal signatures" of quantum chaos. Eugene Wigner, from his study of the eigenspectra of the Hamiltonian matrices corresponding to the compound nuclei of atoms, hypothesized that the fluctuations in these eigenspectra must be related to the fluctuations in the eigenspectra of large matrices (subject to some symmetry conditions) whose entries are random numbers. This profound hypothesis resulted in the development of Random Matrix Theory (RMT), which has scope for application in any discipline involving the study of stochastic processes.

If the entries of a random matrix are Gaussian distributed random numbers, then that random matrix belongs to the Gaussian ensemble of random matrices. A Gaussian orthogonal ensemble matrix is symmetric and its entries are real numbers. A Gaussian unitary ensemble matrix is Hermitian and its entries are complex numbers. A Gaussian sympletic ensemble matrix is self-dual and its entries are quaternions. The Hamiltonian matrices of many quantum Hamiltonian systems belong to one of these ensembles. From the study of the phases of the eigenvalues of unitary random matrices, circular ensembles of random matrices have be defined. These ensembles are described as "circular" since these are ensembles of unitary matrices; the eigenvalues of a unitary matrix are uniformly distributed on a circle of unit radius in the Argand plane. The Floquet matrices of quantum Hamiltonian systems belong to one of these ensembles.

The characteristics of the dynamics of a quantum system can be inferred only from its observables. The normalised probability distribution of the distance between the phases of the eigenvalues of the Floquet matrix of a quantum system (arranged in increasing order and scaled by the their average) provides information on the dynamics of the system (level spacing distribution) [4][5]:

- If this distribution is Poissonian, then the system exhibits regular behaviour.
- If this distribution is Wigner-Dyson, then the system exhibits chaotic behaviour.

Chapter 3

Kicked Rotor System

Simple Hamiltonian systems have been important models in chaos and quantum chaos. A periodically kicked Hamiltonian systems is described by a Hamiltonian that is periodic with time. Simple periodically kicked Hamiltonian systems are special. A simple periodically kicked Hamiltonian system is the kicked rotor system. The Hamiltonian describing the kicked rotor system is:

$$H(t) = \frac{L^2}{2I} + k\cos(\theta)\delta_\tau(t)$$

where L is its angular momentum, I is its moment of inertia and k is the amplitude of the "kick", which is a periodic impulse represented by:

$$\delta_\tau(t) = \sum_{n=0}^{\infty} \delta(t - n\tau)$$

where τ is the kicking time period. The Hamilton's equations of motion describing its dynamics are:

$$\dot{L} = -\frac{\partial H}{\partial \theta} = k\sin(\theta)\sum_{n=0}^{\infty}\delta(t - n\tau)$$
$$\dot{\theta} = \frac{\partial H}{\partial L} = \frac{L}{I}$$

Let θ_n and L_n be the values of θ and L just before the $(n+1)^{\text{th}}$ kick. Immediately after the $(n+1)^{\text{th}}$ kick, $L \to L_{n+1} = L_n + k\sin(\theta_n)$ while θ is constant. In the interval of time

between two successive kicks L is constant while θ increases linearly with time. Therefore:

$$L_{n+1} = L_n + k\sin(\theta_n)$$
$$\theta_{n+1} = \theta_n + \frac{\tau}{I}L_{n+1}$$

The standard map is:

$$\tilde{L}_{n+1} = \tilde{L}_n + K\sin(\theta_n)$$
$$\theta_{n+1} = \theta_n + \tilde{L}_{n+1}$$

where $\tilde{L}_n = \frac{\tau}{I}L_n$ and $K = \frac{k\tau}{I}$. If $k = 1$ and $\tau = 1$, then $\tilde{L}_n = L_n$ and $K = k$. Henceforth, $k = 1$ and $\tau = 1$.

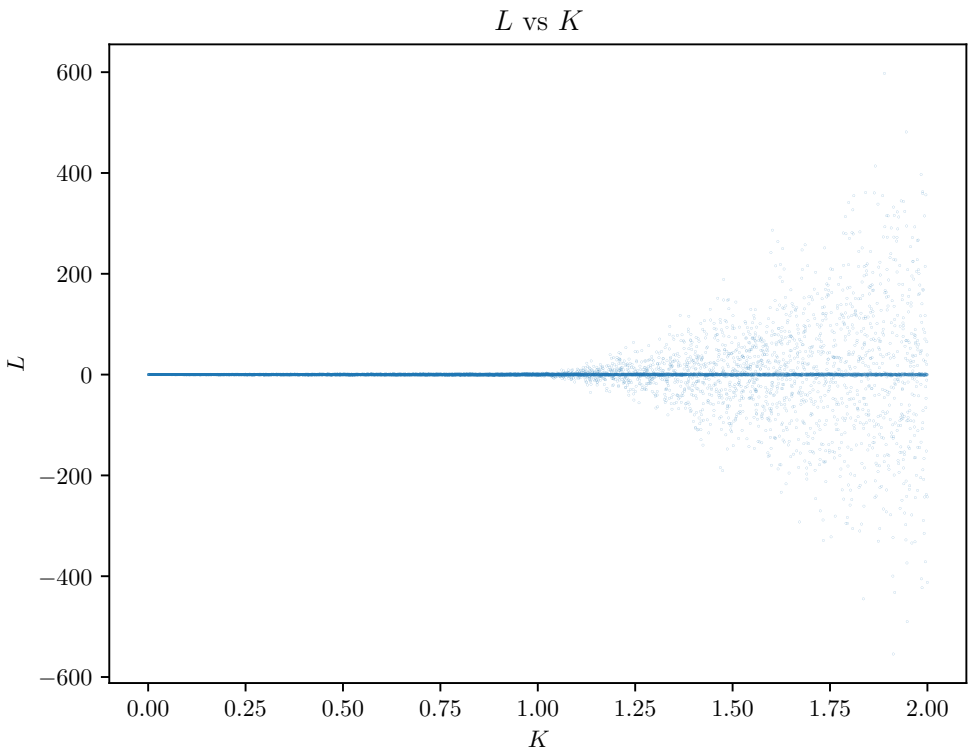

Figure 3.1: This figure contains the plot of $y = L$ vs $x = K$ of the kicked rotor system starting from initial states such that $L_0 = 0$, for $N = 100000$. It can be seen that the values of L begin to deviate from the line $L = 0$ in the neighbourhood of $K = 1$.

The following figures are visual representations of the Poincaré surface section of the kicked rotor system. They contain the plots of $y = (L \mod 2\pi)/2\pi$ vs. $x = (\theta \mod 2\pi)/2\pi$ of the system starting from 10 different initial states such that the points (L_0, θ_0) lie on the line $y = x$, for $N = 1000$.

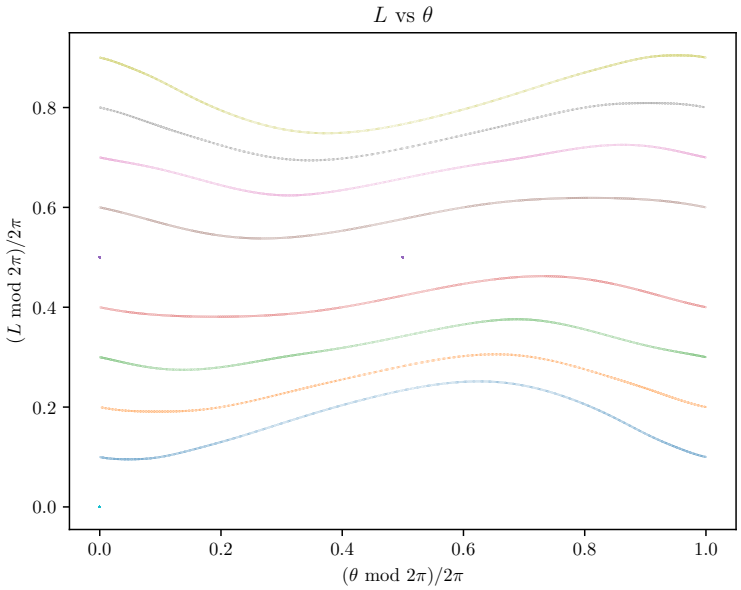

Figure 3.2: For $K = 0.5$, the system exhibits regular behaviour for all initial conditions.

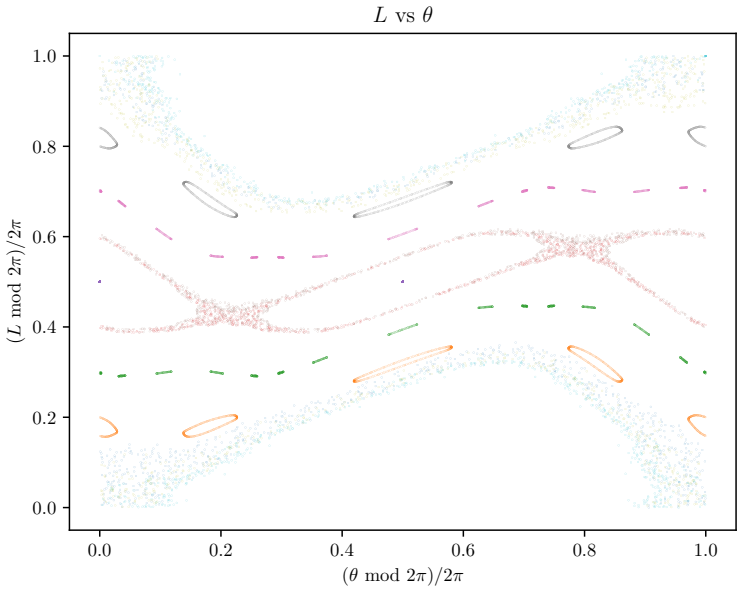

Figure 3.3: For $K = K_c = 0.9716$, the system exhibits chaotic behaviour for many initial conditions.

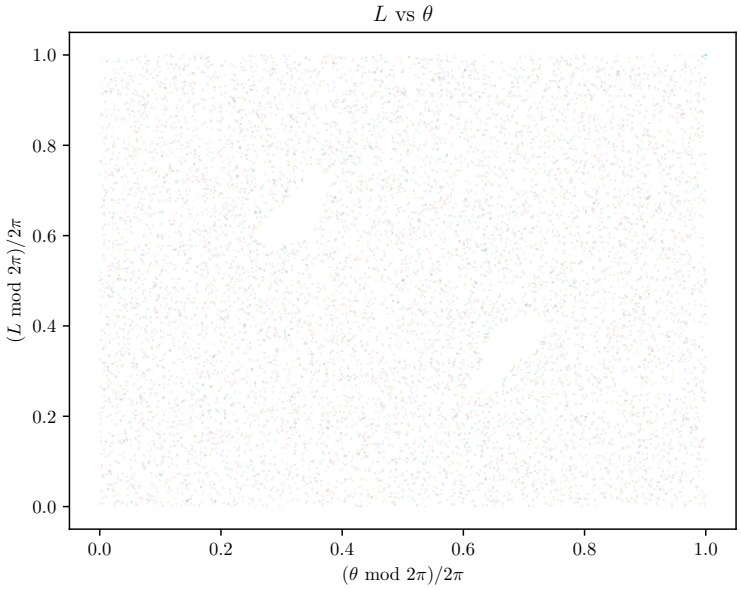

Figure 3.4: For $K = 5.0$, the system exhibits chaotic behaviour for almost all initial conditions.

Let $f_N(\Delta L)$ be the probability that $L_N - L_0 = \Delta L$ after N kicks. Then:

$$\begin{aligned} f_N(\Delta l) &= \langle \delta(\Delta l - (L_N - L_0)) \rangle \\ &= \left\langle \frac{1}{2\pi} \int_{-\infty}^{+\infty} e^{it(\Delta l - (L_N - L_0))} \, \mathrm{d}t \right\rangle \\ &= \left\langle \frac{1}{2\pi} \int_{-\infty}^{+\infty} e^{it\Delta L} \prod_{n=0}^{N-1} \left(e^{-it(L_{n+1} - L_n)} \right) \, \mathrm{d}t \right\rangle \\ &= \left\langle \frac{1}{2\pi} \int_{-\infty}^{+\infty} e^{it\Delta L} \prod_{n=0}^{N-1} \left(e^{-iKt\sin(\theta_n)} \right) \, \mathrm{d}t \right\rangle \end{aligned}$$

where $\langle\rangle$ involves averaging over q random initial conditions; $q \to \infty$. Assumption: For sufficiently large values of K, θ_n are uncorrelated for $t \to \infty$. Then:

$$\begin{aligned} f_N(\Delta L) &= \frac{1}{2\pi} \int_{-\infty}^{+\infty} e^{it\Delta L} \prod_{n=0}^{N-1} \left(\left\langle e^{-iKt\sin(\theta_n)} \right\rangle \right) \, \mathrm{d}t \\ &= \frac{1}{2\pi} \int_{-\infty}^{+\infty} e^{it\Delta L} \prod_{n=0}^{N-1} \left(\frac{1}{2\pi} \int_0^{2\pi} e^{-iKt\sin(\theta_n)} \, \mathrm{d}\theta_n \right) \, \mathrm{d}t \\ &= \frac{1}{2\pi} \int_{-\infty}^{+\infty} e^{it\Delta L} [J_0(Kt)]^N \, \mathrm{d}t \\ &\approx \frac{1}{k\sqrt{\pi N}} e^{-\frac{(\Delta L)^2}{K^2 N}} \qquad \text{(for large } N\text{)} \end{aligned}$$

Let the kicked rotor system start from initial states such that $L_0 = 0$. Assumption: For sufficiently large values of K, θ_n are uncorrelated for $N \to \infty$. Then:

$$\begin{aligned} \langle (L_N - L_0)^2 \rangle = \langle L_N^2 \rangle &= \left\langle K^2 \sum_{n=0}^{N-1} \left(\sum_{n'=0}^{N-1} \sin(\theta_n) \sin(\theta'_n) \right) \right\rangle \\ &\approx K^2 \sum_{n=0}^{N-1} \langle \sin(\theta_n) \rangle = \frac{K^2 N}{2} \qquad \text{(for large } N\text{)} \end{aligned}$$

where $\langle\rangle$ indicates averaging over q random initial conditions; $q \to \infty$.

The following figures contain histograms that represent the normalized probability distribution of the angular momentum of the kicked rotor system starting from initial states such that $L_0 = 0$, for $q = 100000$ and $N = 1000$.

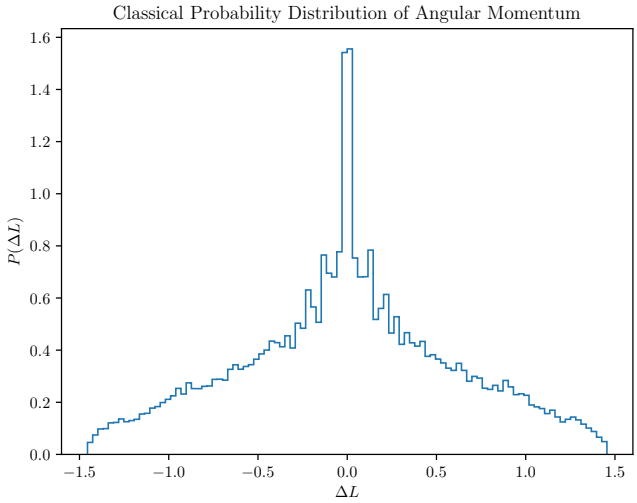

Figure 3.5: For $K = 0.5$, the angular momentum of the system is most probably in the neighbourhood of 0. Higher and lower values of angular momentum are less probably attained by the system.

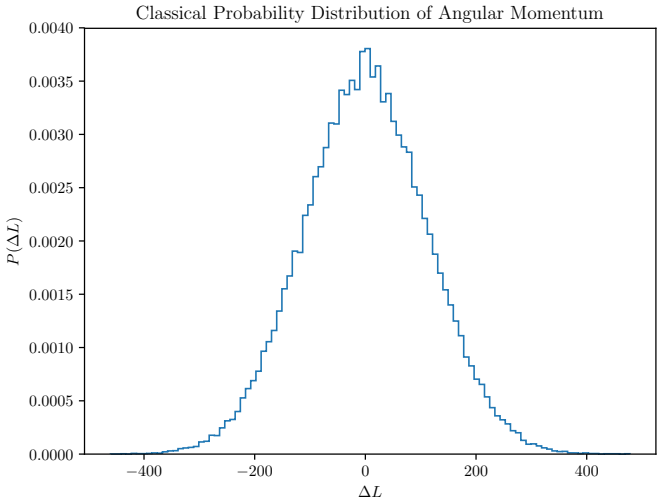

Figure 3.6: For $K = 5.0$, the normalized probability distribution of the angular momentum of the system is Gaussian centred at 0.

The following figures contain the plots of $y = \langle L_N^2 \rangle$ vs. $x = N$ of the kicked rotor system starting from initial states such that $L_0 = 0$, for $q = 10000$ and $N = 1000$. The average energy of the system $\langle E \rangle = \frac{\langle L_N^2 \rangle}{2I}$.

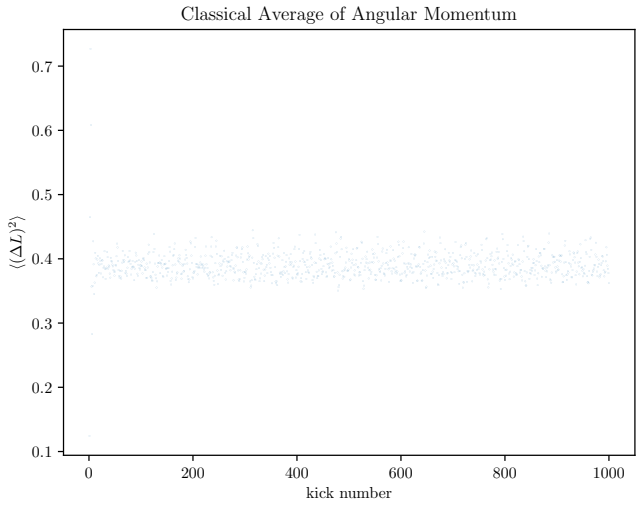

Figure 3.7: For $K = 0.5$, the average energy of the system fluctuates about a saturation value with N and can be considered to be nearly constant.

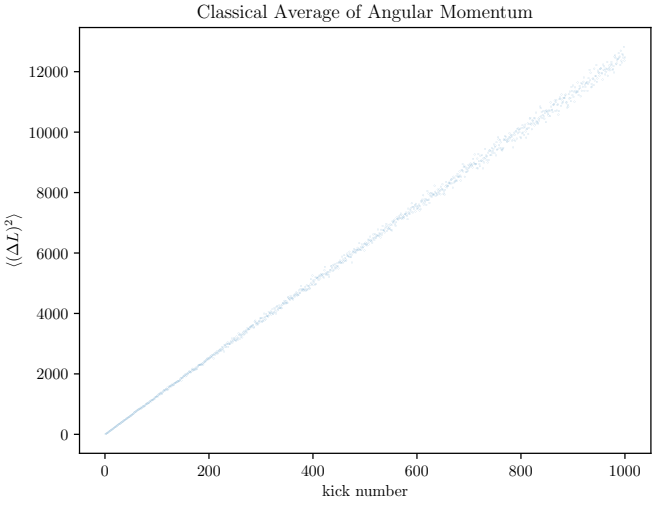

Figure 3.8: For $K = 5.0$, the average energy of the system increases linearly with N (characteristic of a diffusion process).

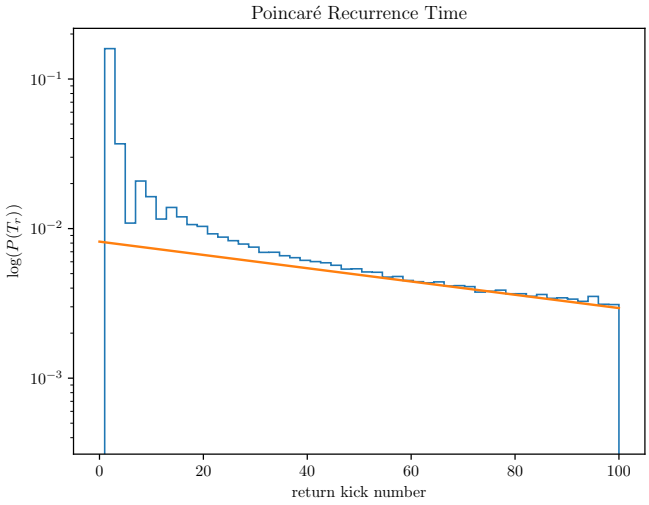

Figure 3.9: This figure contain a histogram that represents the logarithm of the normalized probability distribution of the Poincaré first recurrence times of the kicked rotor system for $K = 5.0$. (No. data points = 100000, Volume of neighbourhood = 1.0). The logarithm of the normalized probability distribution of the Poincaré first recurrence times of the system decreases linearly with return kick number for sufficiently large return kick numbers.

Summary

- For sufficiently small values of K, the kicked rotor system exhibits regular behaviour. For values of $K > (K_c \approx 0.9716)$, it exhibits chaotic behaviour.

- For values of $K > K_c$, the normalized probability distribution of the angular momentum of the kicked rotor system is Gaussian centred at 0, for $q \to \infty$ and $N \to \infty$. This was expected from the theoretical calculation.

- For values of $K > K_c$, the variance of the angular momentum of the kicked rotor system increases linearly with N, for $q \to \infty$ and $N \to \infty$. This was expected from the theoretical calculation.

- For sufficiently large Poincaré recurrence times, $\log(P(T_r)) = -T_r + const.$. This was expected from the theory.

3.1 Quantum Kicked Rotor System

The Hamiltonian describing the quantum kicked rotor (QKR) system is:

$$\hat{H}(t) = \frac{\hat{L}^2}{2I} + k\cos(\hat{\theta})\delta_\tau(t)$$

with the commutation relation:

$$[\hat{\theta}, \hat{L}] = i\hbar\hat{I}$$

Here:

$$\hat{H}_0 = \frac{\hat{L}^2}{2I}; \quad \hat{V}(t) = \hat{V}_0\delta_\tau(t)$$

where:

$$\hat{V}_0 = k\cos(\hat{\theta}); \quad \delta_\tau(t) = \sum_{n=0}^{\infty}\delta(t - n\tau)$$

A modified quantum Hamiltonian system is constructed by replacing the impulse in $\hat{H}(t)$ with a pulse having finite time width $\Delta\tau$ and finite height $1/\Delta\tau$ [6]. The Hamiltonian describing this system is:

$$\begin{cases} \hat{H}_0 & \text{when } q\tau < t < (q+1)\tau - \Delta\tau \\ \hat{H}_0 + \dfrac{\hat{V}_0}{\Delta\tau} & \text{when } (q+1)\tau - \Delta\tau < t < (q+1)\tau \end{cases}$$

This Hamiltonian is piece-wise constant. Therefore, the time evolution operator $\hat{W}(t)$ of this system for $t \in [0, \tau - \Delta\tau)$ is:

$$\hat{W}(t) = e^{-\frac{i}{\hbar}\hat{H}_0 t}$$

and for $t \in [\tau - \Delta\tau, \tau)$ is:

$$\hat{W}(t) = e^{-\frac{i}{\hbar}\left(\hat{H}_0 + \frac{\hat{V}_0}{\Delta\tau}\right)(t-(\tau-\Delta\tau))}\hat{W}(\tau - \Delta\tau)$$

Therefore, the Floquet operator of this system is:

$$\hat{W}(\tau) = e^{-\frac{i}{\hbar}\left(\hat{H}_0 + \frac{\hat{V}_0}{\Delta\tau}\right)(\Delta\tau)}e^{-\frac{i}{\hbar}\hat{H}_0(\tau-\Delta\tau)}$$

and the Floquet operator of the QKR system is:

$$\hat{U}(\tau) = \lim_{\Delta\tau \to 0} \hat{W}(\tau) = e^{-\frac{i}{\hbar}\hat{V}_0} e^{-\frac{i}{\hbar}\hat{H}_0 \tau}$$

A complete set of orthonormal eigenstates of $\hat{L}$ is $\{|n\rangle \leftrightarrow \frac{1}{\sqrt{2\pi}} e^{in\theta}\}$. The entries of the Floquet matrix of the QKR system, expressed using $\{|n\rangle\}$ are:

$$\begin{aligned}
[\mathbf{U}(\tau)]_{mn} &= \langle m| \hat{U}(t) |n\rangle \\
&= \int_0^{2\pi} e^{-im\theta} e^{-\frac{ik\cos(\hat{\theta})}{\hbar}} e^{-\frac{i\tau \hat{L}^2}{2\hbar I}} e^{in\theta} \, \mathrm{d}\theta \\
&= i^{n-m} e^{-\frac{i\hbar\tau n^2}{2I}} J_{n-m}\left(\frac{k}{\hbar}\right)
\end{aligned}$$

where $J_\alpha(x)$ is the Bessel function of the first kind of order α. In this basis, only the entries of $\mathbf{U}(\tau)$ close to its diagonal entries are significant. Let $|A(0)\rangle$ be the initial state (angular momentum ground state) of the QKR system. Then:

$$|A(N\tau)\rangle = \mathbf{U}^N |A(0)\rangle$$

The expectation value of $\hat{L}^2$ for $|A(N\tau)\rangle$ is:

$$\langle \hat{L}^2 \rangle_N = \langle A(N\tau)| \mathbf{L}^2 |A(N\tau)\rangle$$

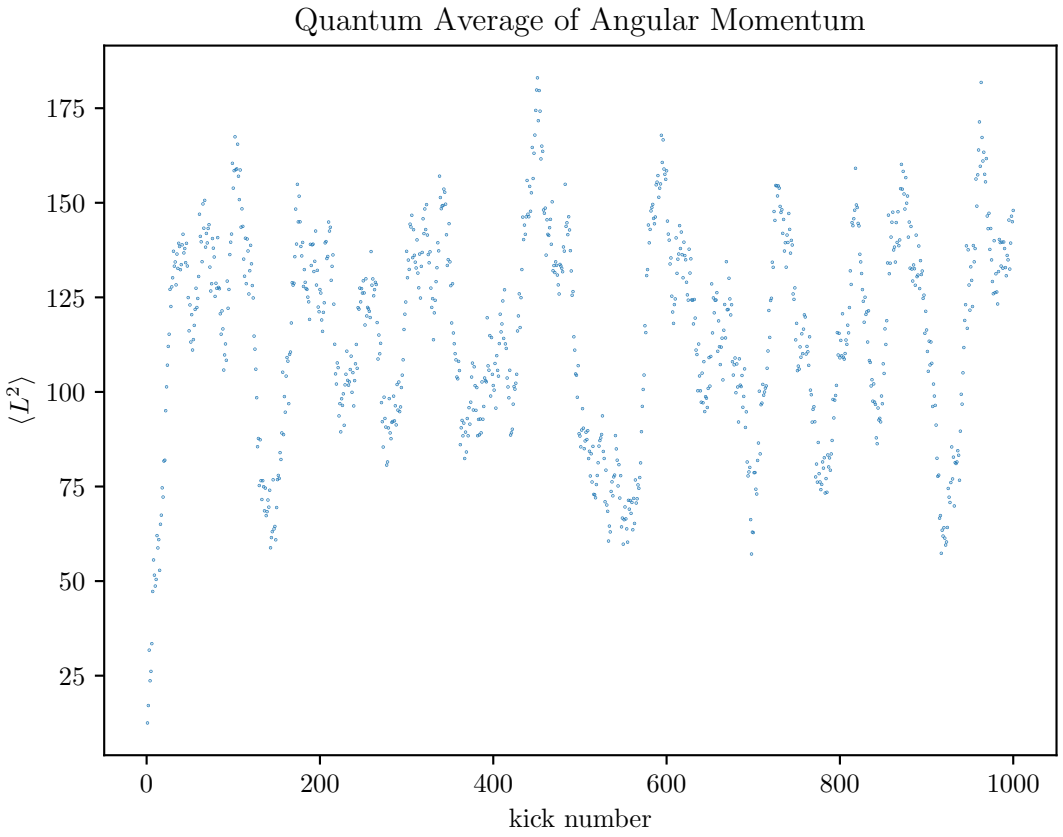

Figure 3.10: This figure contains the plot of $y = \langle \hat{L}^2 \rangle_N$ vs. $x = N$ (kick number) of the QKR system starting from the aforementioned initial state $|A(0)\rangle$ for $K = 5.0$

Classically, the kicked rotor system exhibits chaotic behaviour for values of $K > K_c$ and the variance of its angular momentum ($\propto$ energy) increases linearly with time. However, the expectation value of $\hat{L}^2$ of the QKR system increases with time till a value of time (break time) after which it fluctuates about a particular finite value, implying that the system has undergone a transition of state from a regime in which it exhibits chaotic behaviour to a regime in which it exhibits regular behaviour. "The QKR system has localized."

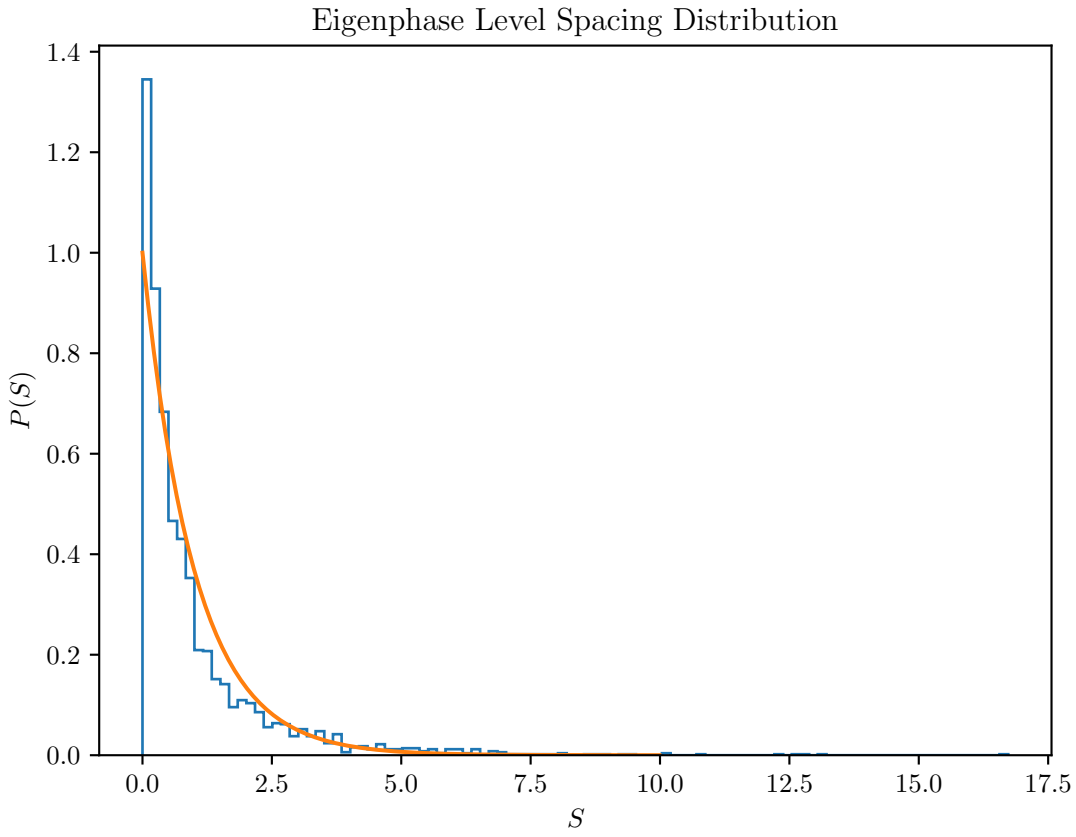

Figure 3.11: This figure contains a histogram that represents the level spacing distribution of the QKR system for $K = 100$. It can be seen that the distribution is nearly Poissonian ($\propto e^{-S}$). For this result, the order of the Floquet matrix of the QKR system is 2001×2001; an exact fit is expected if its order is much larger and its elements are more precisely evaluated and if the bin size of the histogram is smaller.

Note: The Floquet matrix has infinite order. Therefore, for the purpose of numerical calculations, it must be truncated.

- If the QKR system localizes, then the numerical calculations using its truncated Floquet matrix will be effective even for large N.
- If the QKR system delocalizes, then the numerical calculations using its truncated Floquet matrix will be effective till a particular value of N.

To know more about the original work, refer to [7][8][9].

Chapter 4

Anderson Localization

Quantum localization is the localization of the dynamics of a quantum system in its phase space. The study of localization of the QKR system is facilitated by the existence of a mapping from the QKR system to the model of an electron moving in a one-dimensional disordered lattice i.e the one-dimensional Anderson model with on-site disorder [10].

Let $t = s\tau$. Then the Schrödinger equation describing the dynamics of the QKR system is:

$$i\frac{\partial\tilde{\psi}(s)}{\partial s} = -\frac{\hbar^2\tau}{2\hbar I}\frac{\partial^2\tilde{\psi}(s)}{\partial\theta^2} + \frac{k}{\hbar}\cos(\hat{\theta})\delta_n(s)\tilde{\psi}(s)$$

$$i\frac{\partial}{\partial s}\left|\tilde{\psi}(s)\right\rangle = \left(\mathbf{H}_0' + \mathbf{V}_0'\delta_n(s)\right)\left|\tilde{\psi}(s)\right\rangle \tag{4.1}$$

$$\delta_n(s) = \sum_{n=0}^{\infty}\delta(s-n)$$

where $\mathbf{H}_0'$ is the matrix corresponding to the operator $-\frac{\hbar^2\tau}{2\hbar I}\frac{\partial^2}{\partial\theta^2}$ and $\mathbf{V}_0'$ is the matrix corresponding to the operator $\frac{k}{\hbar}\cos(\hat{\theta})$. For $t \in [N\tau, (N+1)\tau]$:

$$\left|\psi((N+1))\right\rangle = e^{-i\mathbf{H}_0}e^{-i\mathbf{V}_0}\left|\psi(N)\right\rangle$$

Assumption: the following vectors are solutions of 4:

$$\left|\psi(N)\right\rangle = e^{-i\omega_\alpha N}\left|u_\alpha(N)\right\rangle$$

where:

$$|u_\alpha(N+1)\rangle = |u_\alpha(N)\rangle$$

where $\omega_\alpha = \Omega_\alpha \tau/\hbar$. Then:

$$|u_\alpha(N)\rangle = e^{-i(\mathbf{H}_0 - \omega_\alpha I)} e^{-i\mathbf{V}_0} |u_\alpha(N)\rangle$$

Define:

$$\mathbf{T}_\alpha \coloneqq \tan((\mathbf{H}_0 - \omega_\alpha I)/2); \quad \mathbf{W} \coloneqq \tan(\mathbf{V}_0/2); \quad |v_\alpha(N)\rangle \coloneqq (I + i\mathbf{W})^{-1} |u_\alpha(N)\rangle$$

Then:

$$(\mathbf{T}_\alpha + \mathbf{W}) |v_\alpha(N)\rangle = 0$$

Let $\{|n\rangle\}$ be a complete set of orthonormal eigenstates of $\hat{L}$. Then:

$$\langle n| \mathbf{T}_\alpha |v_\alpha(N)\rangle + \langle n| \mathbf{W} |v_\alpha(N)\rangle = 0$$

$$\sum_{n=-\infty}^{\infty} \langle n| \mathbf{T}_\alpha |n\rangle \langle n|v_\alpha(N)\rangle + \sum_{m=-\infty}^{\infty} \langle n| \mathbf{W} |m\rangle \langle m|v_\alpha(N)\rangle = 0$$

$$\boxed{T_n(\alpha) v_n(\alpha) + \sum_{m=-\infty\,(\neq n)}^{\infty} W_{nm} v_m(\alpha) = -W_{nn}(\alpha) v_n(\alpha)}$$

The eigenstates of the Floquet operator of the QKR system have been represented similar to the eigenstates of an electron in the one-dimensional tight-binding model with random disorder in the on-site energy (Anderson model). The major difference between the QKR system and the Anderson model is that, a localization of the expectation value of the angular momentum of the QKR system is observed while a localization of the expectation values of the position of an electron in the Anderson model is observed [11].

Many experiments have been performed on hydrogen atoms [12][13] in microwave fields and ultra-cold atoms [14][15] in optical lattices to support the results obtained from the theoretical/numerical studies of the QKR system. Localization of the QKR system and other simple quantum Hamiltonian systems has been experimentally observed. Variants of the kicked rotor system have also been studied in many topics: metal-insulator transitions, control of decoherence, measures of entanglement, quantum resonances and quantum transport to quote a few.

Chapter 5

Coupled Kicked Rotors

It is now known that the two-dimensional Anderson model localizes. Knowing the great scope of the kicked rotor system, one can ask the question: "What can be inferred from the study of the dynamics of a system coupled kicked rotors?"

Studies of systems of two coupled kicked rotors have been presented in [16][17][18][19]; more recently in [20]. The variant of a system of two coupled kicked rotors studied in this thesis was presented by the authors of [20]. This variant is a simple and intuitive extension of the system of two identical, independently kicked rotors.

The simplest system of coupled kicked rotors is a system of two coupled kicked rotors. The Hamiltonian describing a system of two coupled kicked rotors is:

$$H(t) = \frac{L_1^2}{2I_1} + \frac{L_2^2}{2I_2} + V(\theta_1, \theta_2)\delta_\tau(t)$$

where L_1, I_1, L_2, I_2 are the angular momentum and the moment of inertia of the first and the second rotors respectively and:

$$\delta_\tau(t) = \sum_{n=0}^{\infty} \delta(t - n\tau)$$

where τ is the kicking time period. For the purpose of this thesis, a variant of this system was studied. This variant has already been studied [20]. The chosen variant is described by

the Hamiltonian:

$$H(t) = \frac{L_1^2}{2I} + \frac{L_2^2}{2I} + k[\cos(\theta_1) + \cos(\theta_2) - \epsilon\cos(\theta_1 - \theta_2)]\delta_\tau(t)$$

where $I_1 = I_2 = I$, k is the amplitude of the kick and ϵ is the coupling strength. The aim is to study the dynamics of this system (TCKR system) for various values of k. The Hamilton's equations of motion describing the dynamics of the TCKR system are:

$$\dot{\theta_1} = \frac{\partial H}{\partial L_1}; \quad \dot{\theta_2} = \frac{\partial H}{\partial L_2}$$
$$\dot{L_1} = -\frac{\partial H}{\partial \theta_1}; \quad \dot{L_1} = -\frac{\partial H}{\partial \theta_1}$$

The iterative map is:

$$L_{1,n+1} = L_{1,n} + K[\sin(\theta_{1,n}) - \epsilon\sin(\theta_{1,n} - \theta_{2,n})] \tag{5.1}$$
$$L_{2,n+1} = L_{2,n} + K[\sin(\theta_{2,n}) - \epsilon\sin(\theta_{2,n} - \theta_{1,n})] \tag{5.2}$$
$$\theta_{1,n+1} = \theta_{1,n} + L_{1,n+1} \tag{5.3}$$
$$\theta_{2,n+1} = \theta_{2,n} + L_{2,n+1} \tag{5.4}$$

where $K = \frac{k\tau}{I}$. If $I = 1$ and $\tau = 1$, then $K = k$. Henceforth, $I = 1, \tau = 1, \epsilon = 1$. Since $H(t)$ is invariant under the exchange $\theta_1 \leftrightarrow \theta_2$, the characteristics of the dynamics of both the rotors are identical. Therefore, only information about L_1 and θ_1 is presented henceforth.

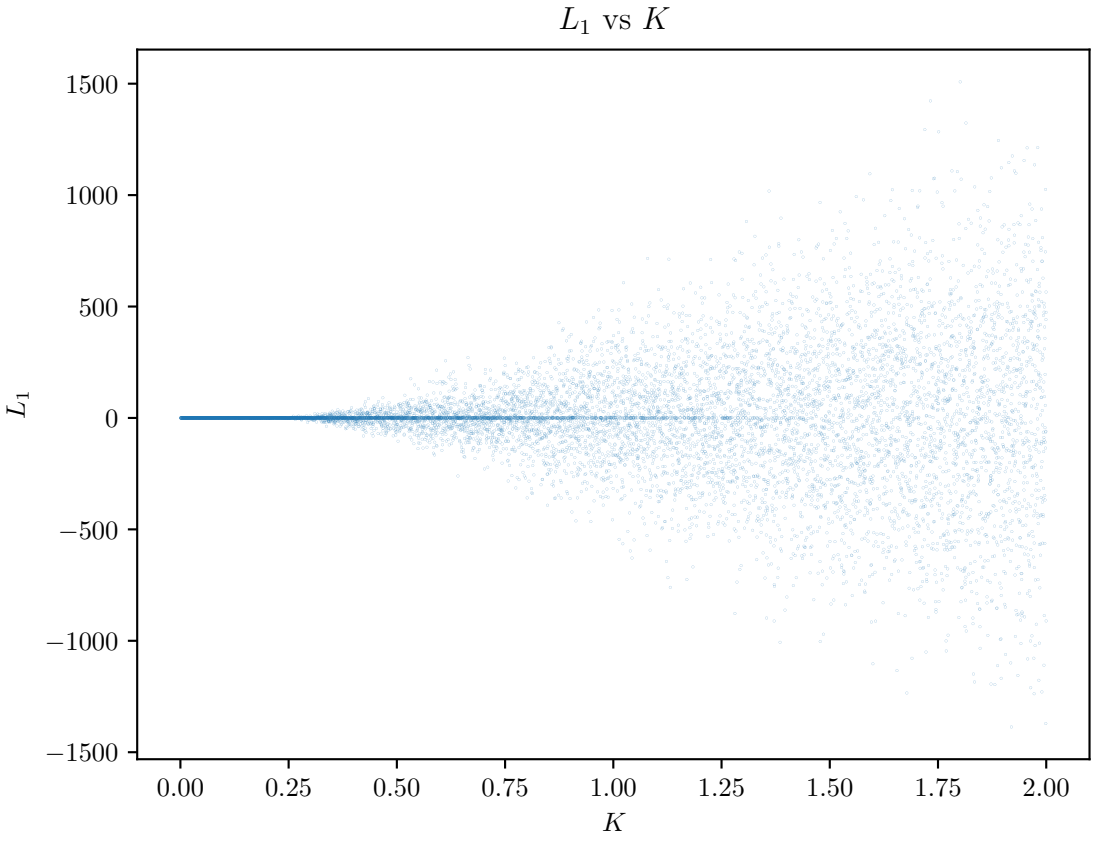

Figure 5.1: This figure contains the plot of $y = L_1$ vs $x = K$ of the kicked rotor system starting from initial states such that $L_{1,0} = 0$, for $\epsilon = 2$ and $N = 100000$. It can be seen that the values of L_1 begin to deviate from the line $L_1 = 0$ in the neighbourhood of $K = 0.3$ and completely deviate in the neighbourhood of $K = 1.5$.

The following figures are visual representations of the Poincaré surface section of the TCKR system. They contain the plots of $y = (L_1 \mod 2\pi)/2\pi$ vs. $x = (\theta_1 \mod 2\pi)/2\pi$ of the system starting from 10 different initial states such that the points $(L_{1,0}, \theta_{2,0})$ lie on the line $x = \pi$ and the points $(L_{2,0}, \theta_{2,0})$ lie on the line $y = \pi$, for $N = 1000$.

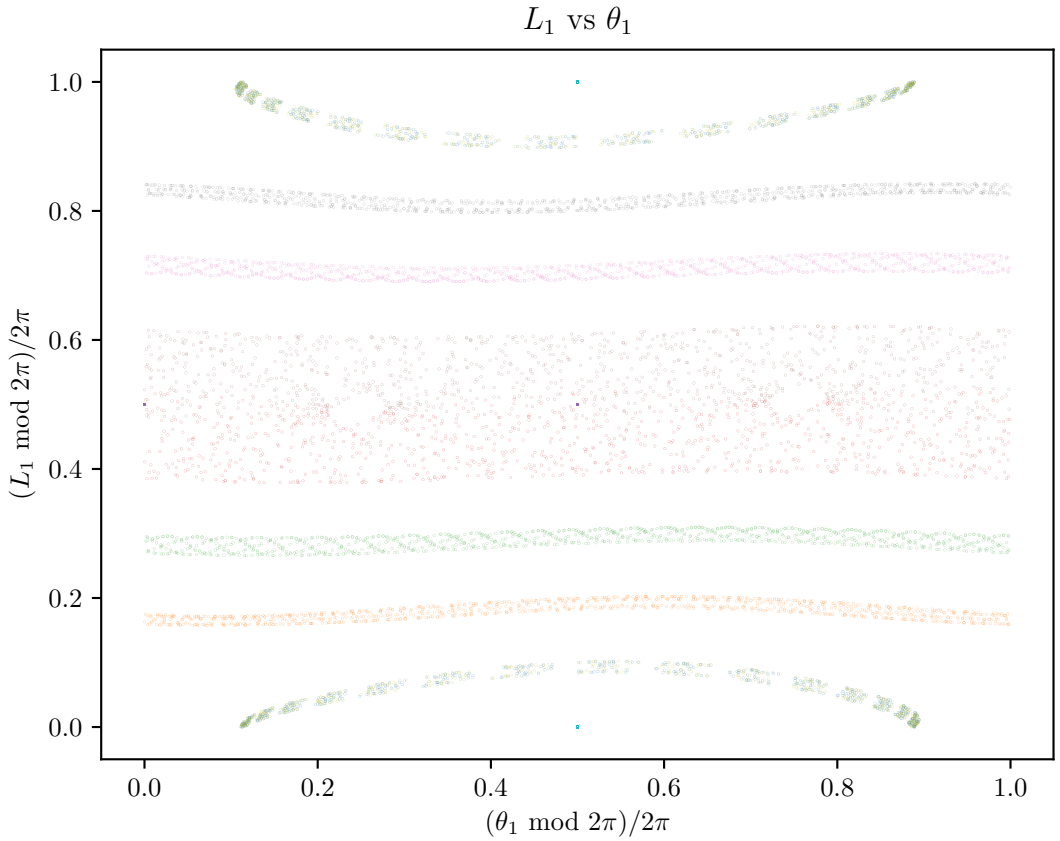

Figure 5.2: For $K = 0.1$, the system exhibits quasi-regular behaviour for most initial conditions. The quasi-regular behaviour can be attributed to the coupling term of the Hamiltonian and the choice of the initial conditions of the system.

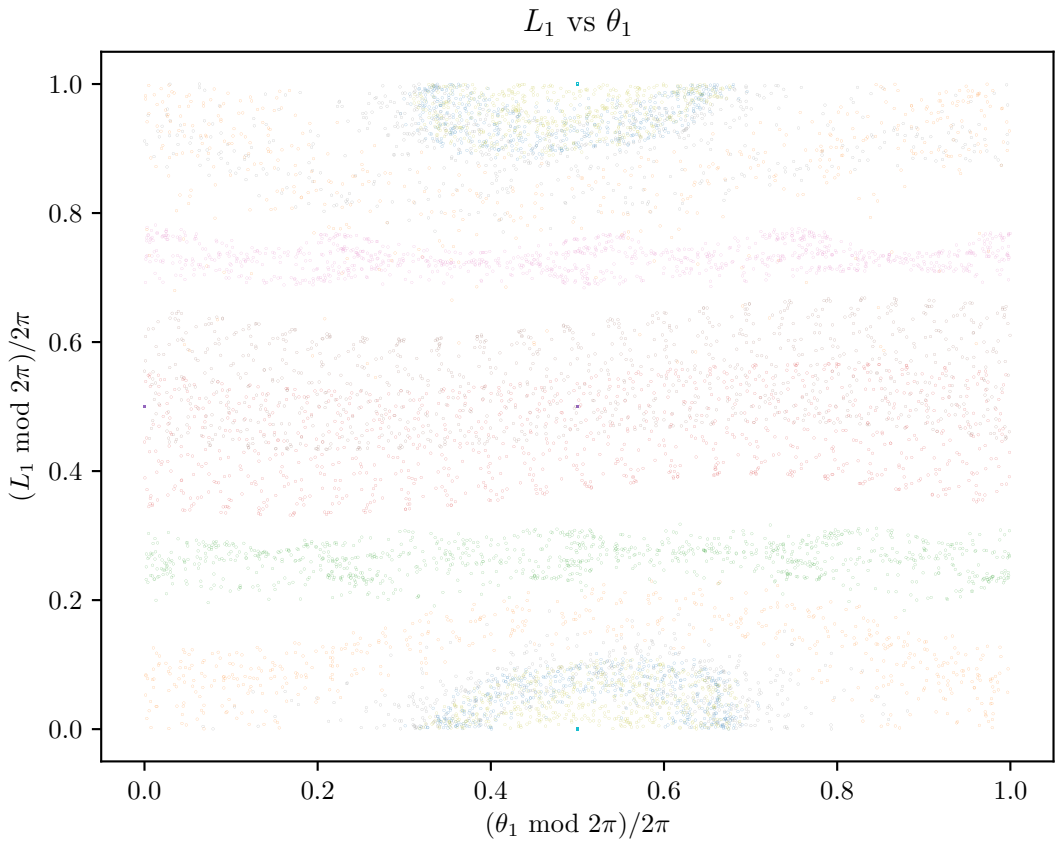

Figure 5.3: For $K = 0.3$, the system exhibits uncharacterised behaviour. Although the system seems to exhibit chaotic behaviour for many initial conditions, there are regions of its phase space inaccessible by it.

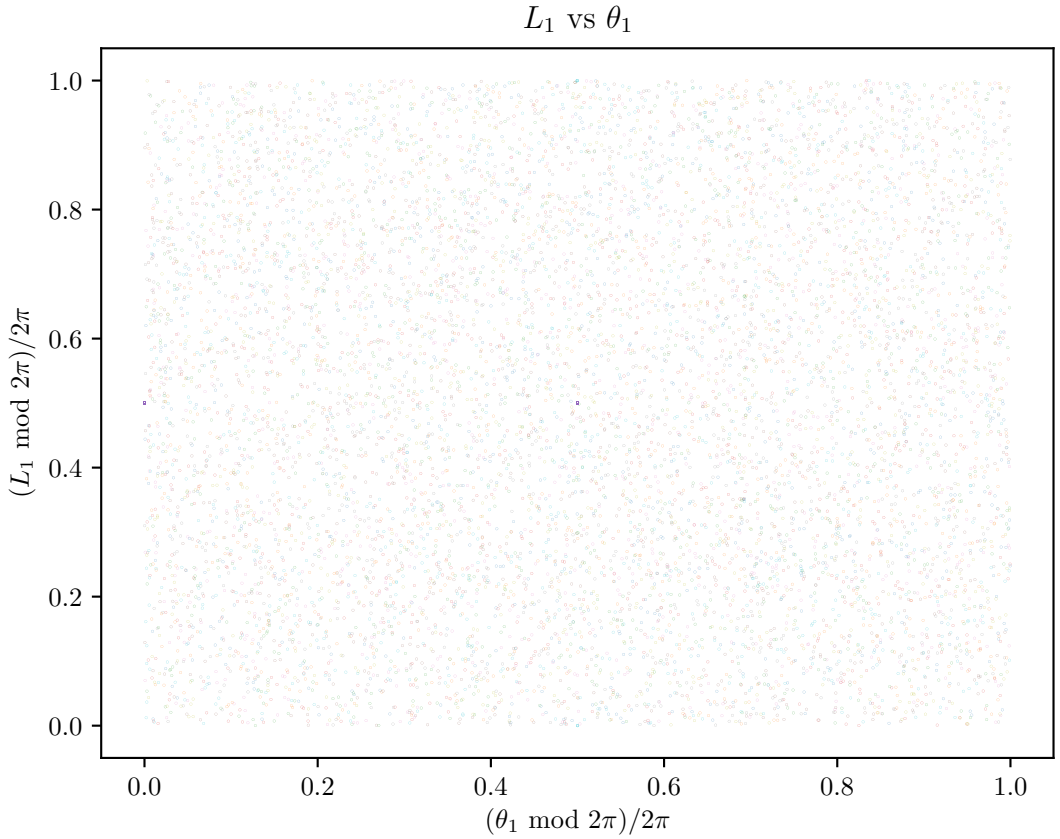

Figure 5.4: For $K = 2.0$, the system exhibits chaotic behaviour for all initial conditions.

The following figures contain histograms that represent the normalized probability distribution of L_1 of the TCKR system starting from initial states such that $L_0 = 0$, for $q = 100000$ and $N = 1000$.

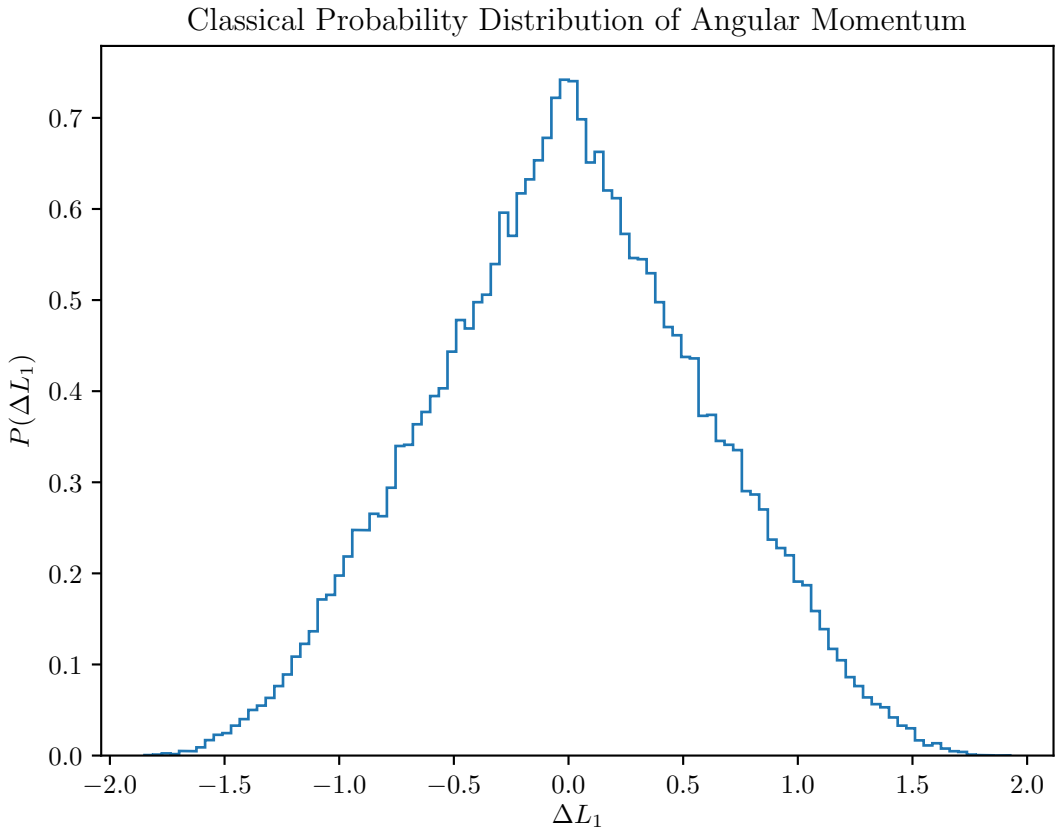

Figure 5.5: For $K = 0.3$, L_1 is most probably in the neighbourhood of 0. Higher and lower values of angular momentum are decreasingly less probably attained by the system.

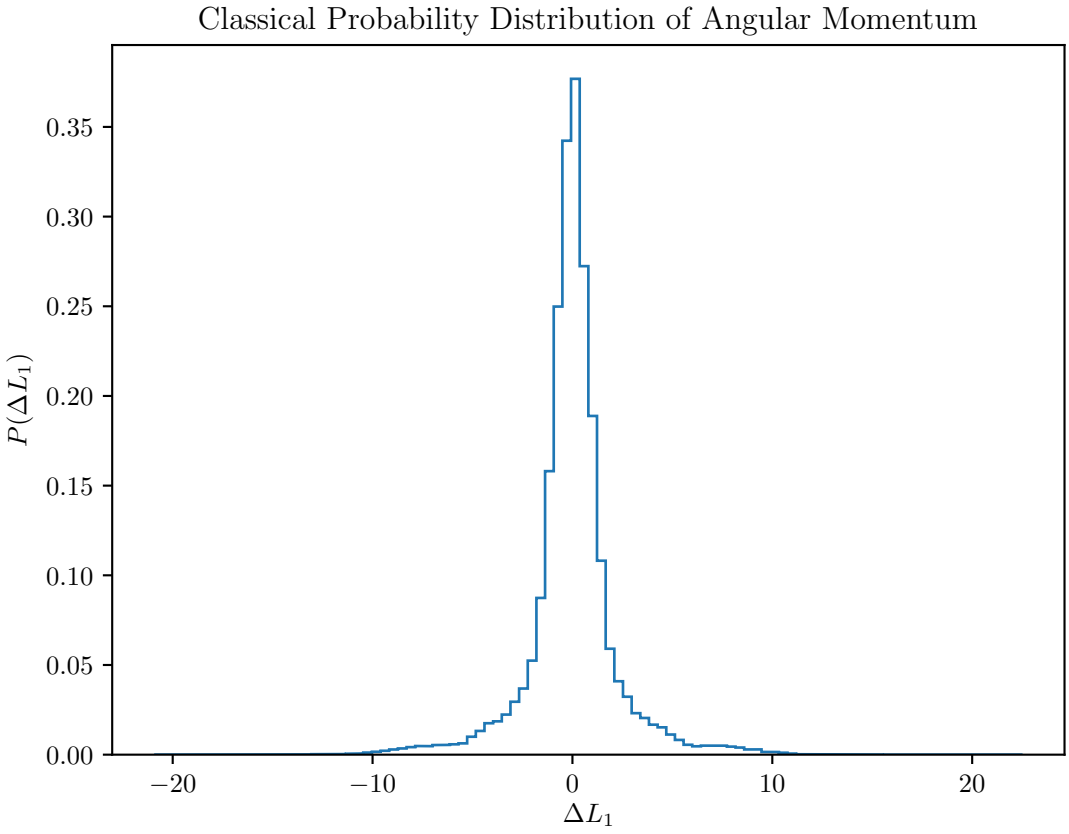

Figure 5.6: For $K = 0.5$, the normalized probability distribution of L_1 peaks at 0 similar to a pulse function.

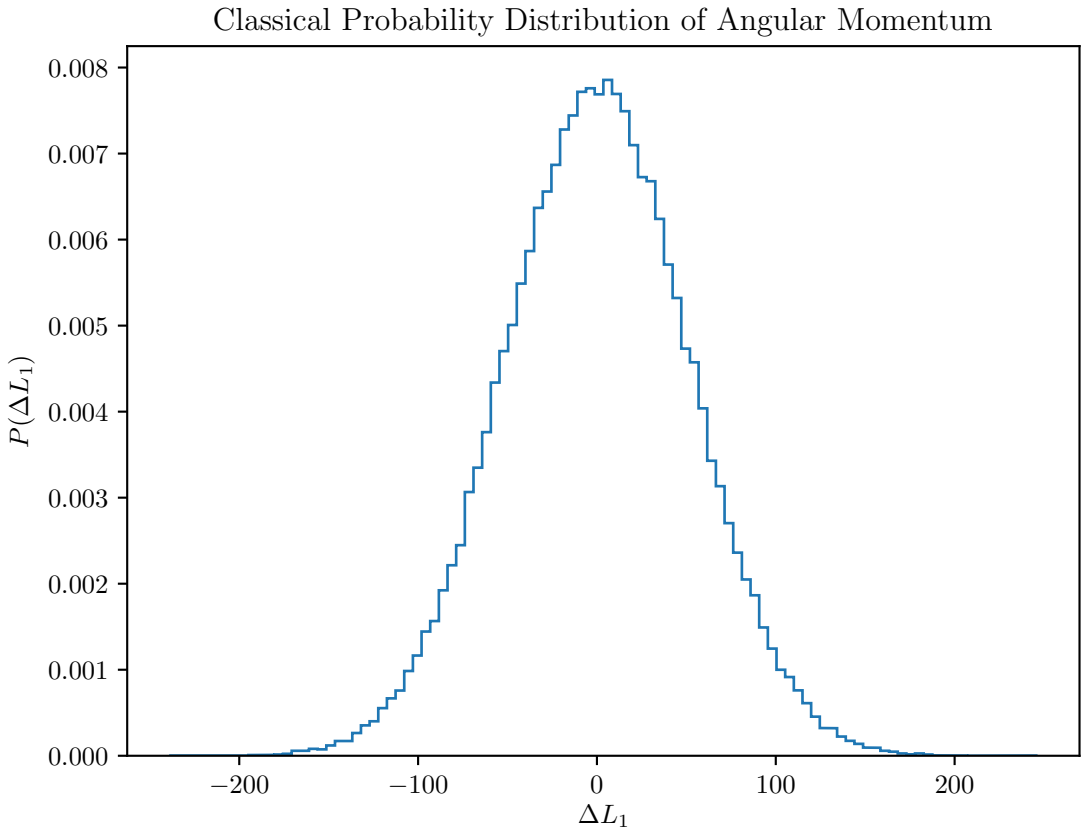

Figure 5.7: For $K = 2.0$, the normalized probability distribution of L_1 is Gaussian centred at 0.

The following figures contain the plots of $y = \langle L_{1,N}^2 \rangle$ vs. $x = N$ of the kicked rotor system starting from initial states such that $L_0 = 0$, for $q = 10000$ and $N = 1000$.

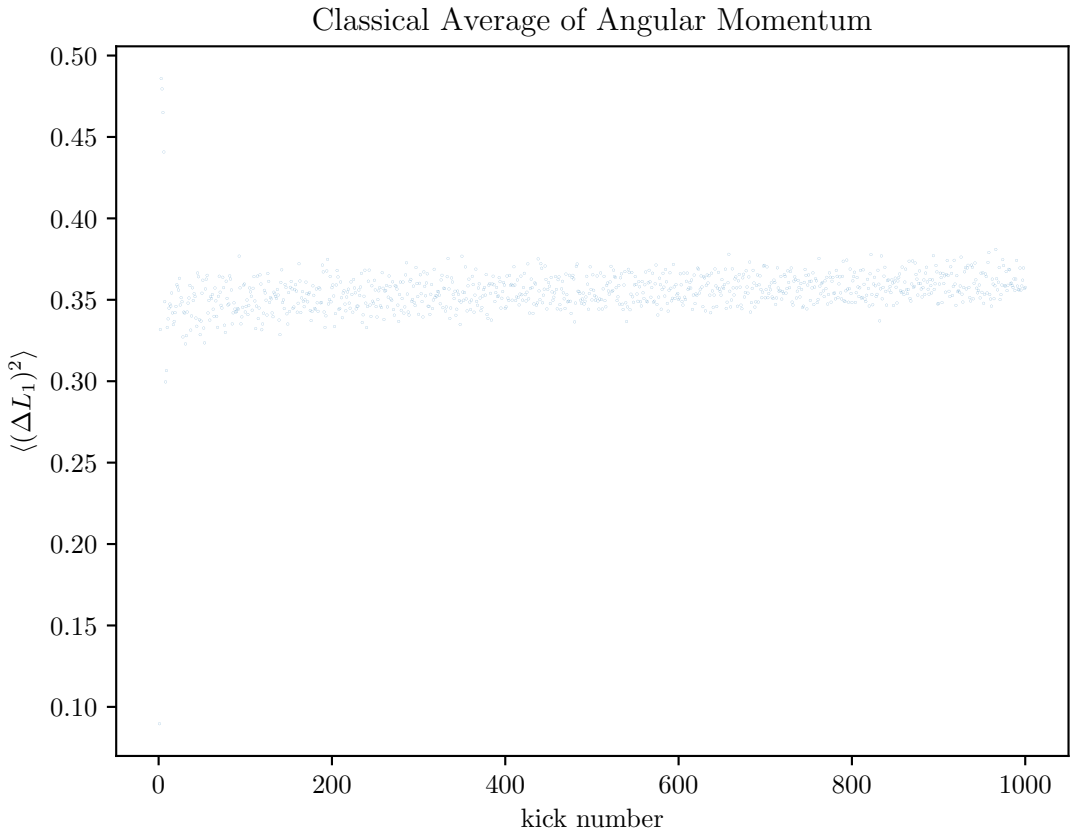

Figure 5.8: For $K = 0.3$, the variance of L_1 fluctuates about a saturation value with N and can be considered to be nearly constant.

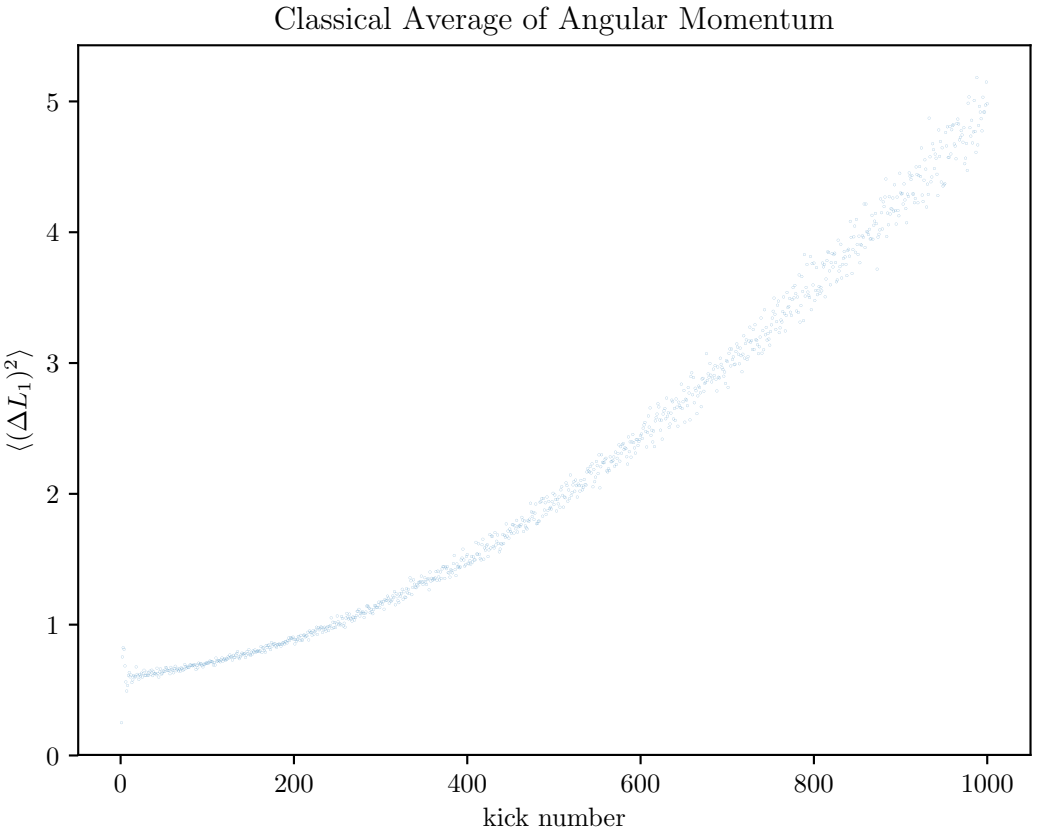

Figure 5.9: For $K = 0.5$, the variance of L_1 increases by a power-law with N.

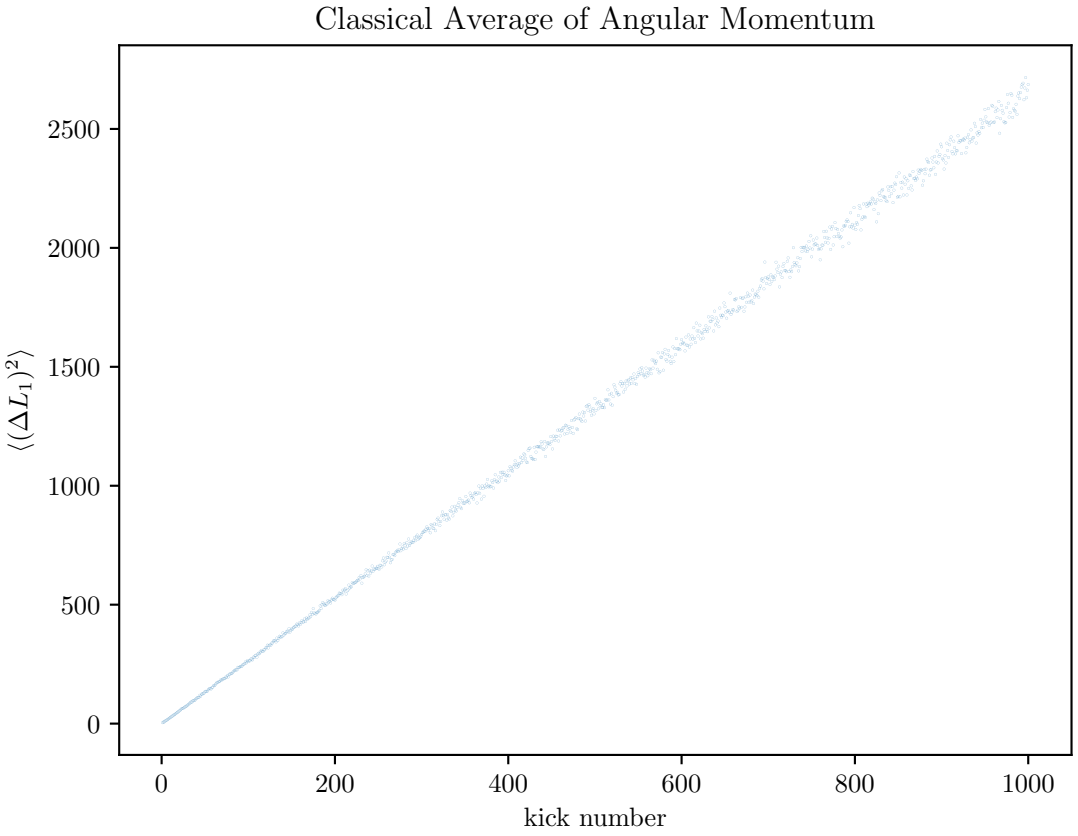

Figure 5.10: For $K = 2.0$, the variance of L_1 increases linearly with N.

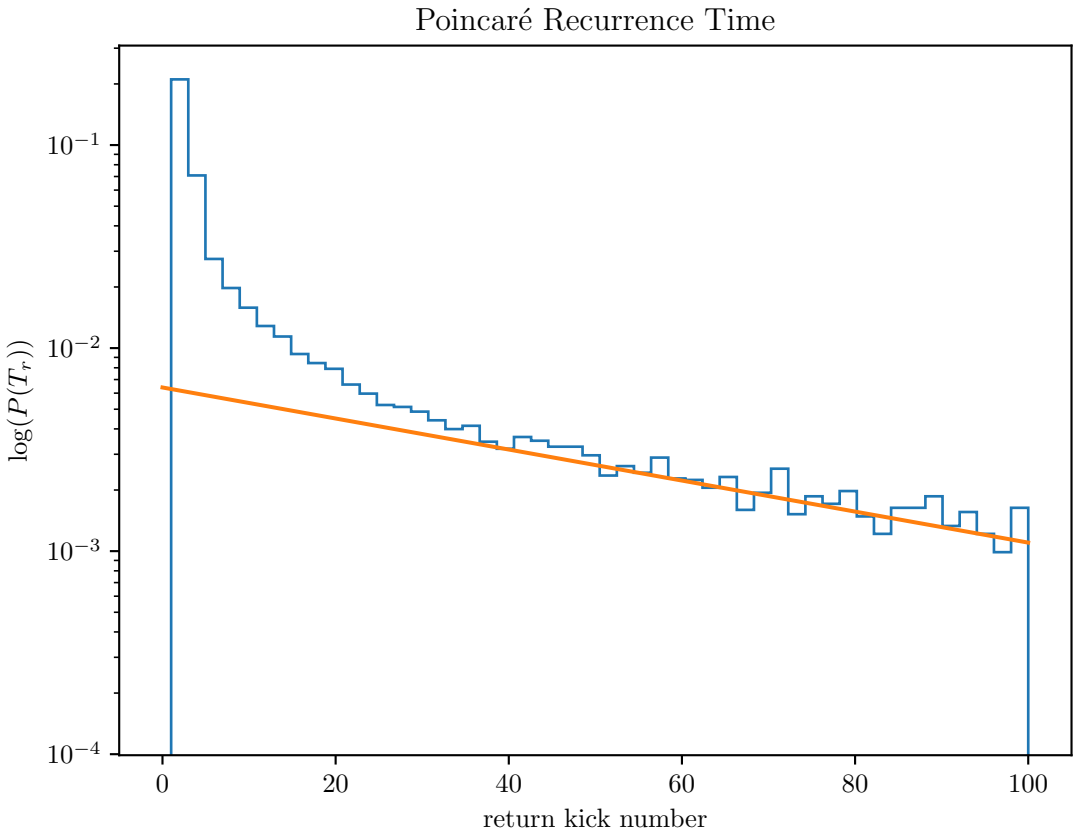

Figure 5.11: This figures contains a histogram that represent the logarithm of the normalized probability distribution of the Poincaré first recurrence times of the TCKR system, for $K = 4.0$. (No. data points = 100000, Volume of neighbourhood = 5.0). The logarithm of the normalized probability distribution of the Poincaré first recurrence times of the system decreases linearly with return kick number for sufficiently large return kick numbers.

Summary

The dynamics of the TCKR system for $K \in [0, 2.0]$ were studied. However, results of the numerical calculations on the system only for few values of K have been presented. It is evident from these figures that:

- The dynamics of TCKR system is very sensitive to its initial conditions. The system

exhibits chaotic mixing.

- The TCKR system undergoes the earlier mentioned transition of state, preliminarily for $K \in [0.3, 0.4]$ and completely for $K \in [1.25, 1.5]$.

- The energy of the TCKR system increases with the kick number, by a power law for $K \in [0.3, 0.4]$ and linearly for $K > 2$.

- The TCKR system is completely chaotic for $K > 2$; for sufficiently large Poincaré recurrence times, $\log(P(T_r)) = -T_r + const.$.

5.1 Quantum TCKR System

The Hamiltonian describing the quantum TCKR system (QTCKR) is:

$$\hat{H}(t) = \frac{\hat{L}_1^2}{2I} + \frac{\hat{L}_2^2}{2I} + k[\cos(\hat{\theta}_1) + \cos(\hat{\theta}_2) - \epsilon\cos(\hat{\theta}_1 - \hat{\theta}_2)]\delta_\tau(t)$$

with the commutation relations:

$$[\hat{\theta}_i, \hat{L}_j] = i\hbar\delta_{ij}\hat{I} \qquad (i, j = 1, 2)$$

The Floquet operator of the QTCKR system is

$$\hat{U}(\tau) = e^{-\frac{ik}{\hbar}\left[\cos(\hat{\theta}_1)+\cos(\hat{\theta}_2)-\cos(\hat{\theta}_1-\hat{\theta}_2)\right]}e^{-\frac{i\tau}{2\hbar I}(\hat{L}_1^2+\hat{L}_2^2)}$$

A complete set of common orthogonal eigenstates of $\hat{L}_1$ and $\hat{L}_2$ is $\{|n_1, n_2\rangle = \frac{1}{2\pi}e^{i(n_1\theta_1+n_2\theta_2)}\}$. The the entries of the Floquet matrix expressed using $\{|n1, n2\rangle\}$ are:

$$\mathbf{U_{m,n}}(\tau) = \frac{1}{4\pi^2}e^{-\frac{i\hbar\tau}{2I}(n_1^2+n_2^2)}\int_0^{2\pi}\int_0^{2\pi} e^{-\frac{i}{\hbar}k[\cos(\hat{\theta}_1)+\cos(\hat{\theta}_2)-\cos(\hat{\theta}_1-\hat{\theta}_2)]}e^{ir_1\theta_1}e^{ir_2\theta_2}\,\mathrm{d}\theta_1\mathrm{d}\theta_2$$

where $r_1 = n_1 - m_1$ and $r_2 = n_2 - m_2$.

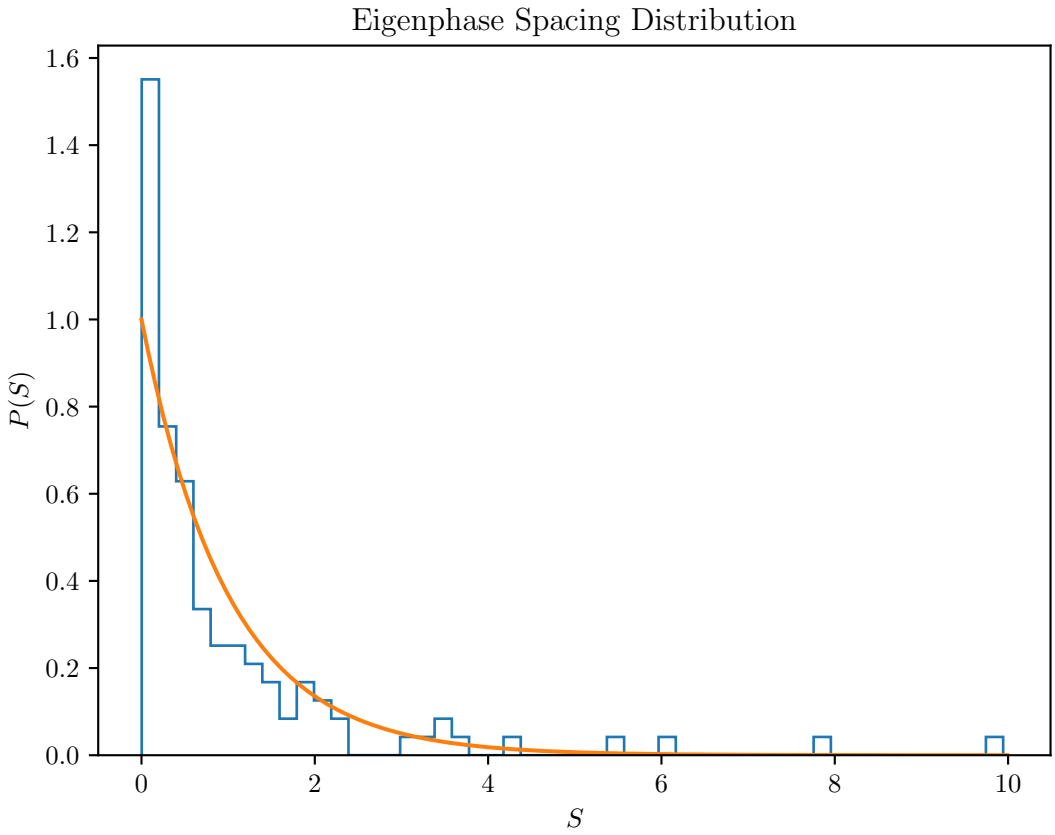

Figure 5.12: This figure contains a histogram that represents the level spacing distribution of the QTCKR system for $K = 10$. It can be seen that the distribution is nearly Poissonian ($\propto e^{-S}$). For this result, the order of the Floquet matrix of the QTCKR system is 441×441; an exact fit is expected if its order is much larger and its elements are more precisely evaluated and if the bin size of the histogram is smaller.

Concluding Remarks

The dynamics of a variant of the general system of two coupled kicked rotors was studied in this thesis using a combination of analytical and numerical techniques. The dynamics of the TCKR system was studied by studying the Poincaré surface sections in its phase space, normalized probability distribution of its angular momentum and the variance of its angular momentum. The normalized probability distribution of the Poicaré recurrence times of the system was also studied. From these studies, it was inferred that the TCKR system undergoes the earlier mentioned transition of state. The dynamics of the QTCKR system was studied by the studying its level spacing distribution. Due to the limitations of the numerical techniques and the computational capabilities available, the maximum order of the truncated Floquet matrix considered was 441×441. However, it is expected that the QTCKR system localizes and this may be tested by considering larger Floquet matrices.

Further research can involve the study of the classical and quantum resonances and the localization-delocalization transitions of this system. The dynamics this system in a finite potential well or external bath can also be studied. A mapping of this system to a two-dimensional Anderson model can be used to enhance the understanding of metal-insulator transitions. Simpler variants of the general system of two coupled kicked rotors can also be studied. Quantized interactions significantly alter the behaviour exhibited by interacting quantum systems. This is an important result for the design of quantum computers and their performances. From an experimental perspective, these systems can be realized in atom-optics experiments, cavity opto-mechanics and NMR experiments. Results from these experiments can then be used to develop high precision sensing equipments and quantum technologies.

Bibliography

[1] Yaroslav I. Boev, Tatiana E. Vadivasova, and Vadim S. Anishchenko. "Poincaré recurrence statistics as an indicator of chaos synchronization". In: *Chaos: An Interdisciplinary Journal of Nonlinear Science* 24 (2014).

[2] Linda Reichl. *The Transition to Chaos: Conservative Classical Systems and Quantum Manifestations*. 2004.

[3] Edward Ott. *Chaos in Dynamical Systems*. Cambrbidge University Press, 2002.

[4] Michael Victor Berry and M. Tabor. "Closed orbits and the regular bound spectrum". In: *Proceedings of the Royal Society of London A: Mathematical and Physical Sciences* 349 (1976).

[5] O. Bohigas, M. J. Giannoni, and C. Schmit. "Characterization of Chaotic Quantum Spectra and Universality of Level Fluctuation Laws". In: *Phys. Rev. Lett.* 52 (1984).

[6] Hans-Jürgen Stöckmann. *Quantum Chaos: An Introduction*. Cambridge University Press, 1999.

[7] D. R. Grempel, R. E. Prange, and Shmuel Fishman. "Quantum dynamics of a nonintegrable system". In: *Phys. Rev. A* 29 (1984).

[8] B.V. Chirikov, F.M. Izrailev, and D.L. Shepelyansky. "Quantum chaos: Localization vs. ergodicity". In: *Physica D: Nonlinear Phenomena* 33 (1988).

[9] Felix M. Izrailev. "Simple models of quantum chaos: Spectrum and eigenfunctions". In: *Physics Reports* 196 (1990).

[10] Shmuel Fishman, D. R. Grempel, and R. E. Prange. "Chaos, Quantum Recurrences, and Anderson Localization". In: *Phys. Rev. Lett.* 49 (1982).

[11] P. W. Anderson. "Absence of Diffusion in Certain Random Lattices". In: *Phys. Rev.* 109 (1958).

[12] E. J. Galvez et al. "Microwave Ionization of H Atoms: Breakdown of Classical Dynamics for High Frequencies". In: *Phys. Rev. Lett.* 61 (1988).

[13] J. E. Bayfield et al. "Localization of classically chaotic diffusion for hydrogen atoms in microwave fields". In: *Phys. Rev. Lett.* 63 (1989).

[14] F. L. Moore et al. "Observation of Dynamical Localization in Atomic Momentum Transfer: A New Testing Ground for Quantum Chaos". In: *Phys. Rev. Lett.* 73 (1994).

[15] F. L. Moore et al. "Atom Optics Realization of the Quantum δ-Kicked Rotor". In: *Phys. Rev. Lett.* 75 (1995).

[16] S. Adachi, M. Toda, and K. Ikeda. "Quantum-Classical Correspondence in Many-Dimensional Quantum Chaos". In: *Phys. Rev. Lett.* 61 (1988).

[17] B. Lévi, B. Georgeot, and D. L. Shepelyansky. "Quantum computing of quantum chaos in the kicked rotator model". In: *Phys. Rev. E* 67 (2003).

[18] Borzumehr Toloui and Leslie E. Ballentine. "Quantum Localization for Two Coupled Kicked Rotors". In: (). arXiv: `0902.0885 [quant-ph]`.

[19] Aydin Cem Keser et al. "Dynamical many-body localization in an integrable model". In: *Phys. Rev. B* 94 (2016).

[20] Simone Notarnicola et al. "From localization to anomalous diffusion in the dynamics of coupled kicked rotors". In: *Phys. Rev. E* 97 (2018).

[21] Boris V Chirikov. "A universal instability of many-dimensional oscillator systems". In: *Physics Reports* 52 (1979).

[22] Michael Tabor. *Chaos and Integrability in Non-linear Dynamics: An Introduction*. John Wiley and Sons, 1989.

[23] R. Shankar. *Principles of Quantum Mechanics*. Springer US, 1994.

[24] Editors: Giulio Casati and Boris Chirikov. *Quantum Chaos: Between Order and Disorder*. Cambridge University Press, 1995.

[25] Fritz Haake. *Quantum Signatures of Chaos*. Springer-Verlag Berlin Heidelberg, 2010.